DESIGN SYNTHESIS AND OPTIMIZATION OF AN ADVANCED SHORT TAKE-OFF AND VERTICAL LANDING (ASTOVL) COMBAT AIRCRAFT

J.P. Fielding, College of Aeronautics, Cranfield University, Cranfield, Bedford MK43 OAL, UK
N. Kehayas, Consultant, 5 Gelonos St., 115 21 Athens, Greece

Abstract

The development of the baseline configuration, the design synthesis and the optimization of the baseline configuration of an advanced short take-off and vertical landing (ASTOVL) combat aircraft are presented. The evaluated baseline configuration is an advanced technology, supersonic STOVL combat aircraft design with an internal weapon bay and powered by a military turbofan with a remote lift system (RLS) for landing. The RLS provides lift for the front of the aircraft and is made of three ducts starting just after the turbine exit position and ending in a nozzle at the undersurface of the aircraft, aft of the nose undercarriage bay. At landing, thrust in the rear part of the aircraft is provided by a pair of swivelling duct nozzles situated either side of the fuselage, aft of the engine position. The design synthesis describes the aircraft baseline configuration in mathematical form, by means of semi-empirical and sometimes analytical design .relationships. The optimization was carried out with the use of an available optimization code. This was designed to solve constrained optimization problems, that is to minimize a function. subject to a number of constraints and upper and lower bounds imposed on designated variables. The combined synthesis and optimization study indicated that the best objective function for the reduction of the aircraft take-off mass was either the aircraft empty mass or the engine mass. The optimized baseline configuration was a 19.8 m, 18.9 t take-off weight combat aircraft. Comparison with other ASTOVL designs indicated considerable similarities. The comparison suggested that, from the design point of view, a separate lift engine might be a better solution than a RLS.

1. Introduction

The need of short take-off and vertical landing capability for future advanced combat aircraft has led to a number of propulsion lift configurations being proposed [1].

In this paper, a remote lift system (RLS) concept has been selected and subsequently used in the design synthesis and optimization of an advanced short take-off and vertical landing (ASTOVL) combat aircraft with an internal weapon bay [2].

This study is based on a design synthesis philosophy developed in the late 1970's by the Defense and Evaluation Research Agency (DERA) [3,4].

The DERA design synthesis philosophy defines an aircraft mathematically, which is then subjected to an optimization under specified constraints. Following the DERA philoshopy a wide range of aircraft types, including combat aircraft [2,5,6] , have been studied.

The objectives of this work were:

a) The evaluation of the aircraft baseline configuration
b) The design synthesis of the baseline configuration
c) The coding of the design synthesis and its interfacing with an optimization code
d) The optimization of the baseline configuration
c) The comparison of the optimized configuration with similar designs

2. Description

2.1. Baseline Configuration

The design of an ASTOVL combat aircraft is a complicated issue where various schools of thought propose markedly different approaches [7,8,9,10]. The configuration that was specified for this study, that of a supersonic ASTOVL combat aircraft with an internal weapon bay, is a very complex one and adds in the difficulties envisaged in the STOVL field.

STOVL configurations are broadly divided into vectored thrust and remote lift concepts [7,9]. Some, to a certain degree, mixed concepts exist, in the sense that remote lift systems can be vectored. Vectored thrust concepts are relatively straightforward. The engine thrust is vectored for landing, and sometimes for take-off, and in forward flight [7]. Remote lift refers to lift provided by some means to a distant, in relation to the engine, position. The remote lift concepts encompass a variety of schemes; from the use of separate engines for landing (and take-off), perhaps a category of its own, to various arrangements for remote lift, either plain or augmented.

From the engine point of view, vectored thrust is favoured. Ward and Lewis [11] suggest that a vectored thrust scheme is much more efficient and offers a better performance than a remote lift one. However, vectored thrust is not always the best choice for supersonic STOVL combat aircraft. Vectored thrust requires the engine to be placed near the centre of gravity of the aircraft and this requirement results in aircraft with big fuselages in the middle; a situation in contrast to the area-ruling needed in supersonic aircraft. Therefore, a remote lift system (RLS) was selected.

The baseline configuration that evolved after several exploratory configurations is shown in Fig. 1.

The wing is swept back, in a medium-to-high position, and trapezoidal in planform. It is a low tapered, low aspect ratio wing and is based on a thin aerofoil section of constant thickness-to-chord ratio along the span. The wing does not have any dihedral or twist. The tail is conventional and is placed low. The fin and tailplane aerofoil sections are identical to the wing.

The engine is a modern military reheated turbofan of the remote lift type when operating in the landing mode. A system of three ducts, used in landing to provide thrust in the front part of the aircraft, starts just after the turbine exit position and ends in a nozzle at the undersurface of the aircraft after the nose undercarriage bay. It is a hot system without any reheat at the nozzle. It is, therefore, a simply remote lift system (RLS) without any augmentation. Three ducts have been adopted, instead of one, in order to reduce the enormous size a single duct would have. The three ducts, one bigger in the middle and two smaller either side (Fig.2), recombine at the front nozzle. This front nozzle has a limited vectoring capability. At landing the thrust in the rear part of the aircraft is not provided by vectoring the engine rear nozzle, but by a pair of swivelling duct nozzles situated either side after the engine position. These two side duct nozzles are positioned vertically during landing and are stowed horizontally in the fuselage during take-off and forward flight. The system of front ducts and nozzle and the side duct nozzles are used only for landing. The engine has a conventional variable geometry rear nozzle for forward flight.

Two S-shaped intake diffusers with rectangular intakes are used. The intakes have a fixed geometry since the aircraft is specified not to exceed Mach 1.6. The cross-section of the intake diffusers slowly changes, especially after they join, to become circular and meet the engine face.

Due to the operation of the RLS nozzle in the front part of the aircraft during landing, the intake diffusers incorporate auxiliary inlets in their upper surface (Fig.1). These are put into operation at landing, when the usual intakes are closed, to avoid hot ingestion.

The nose undercarriage bay is located after the radome. The main undercarriage bay lies flat under the engine gas generator (Fig. 1).

The weapons of the aircraft, comprising four medium and two short range air-to-air missiles or a number of bombs, are carried

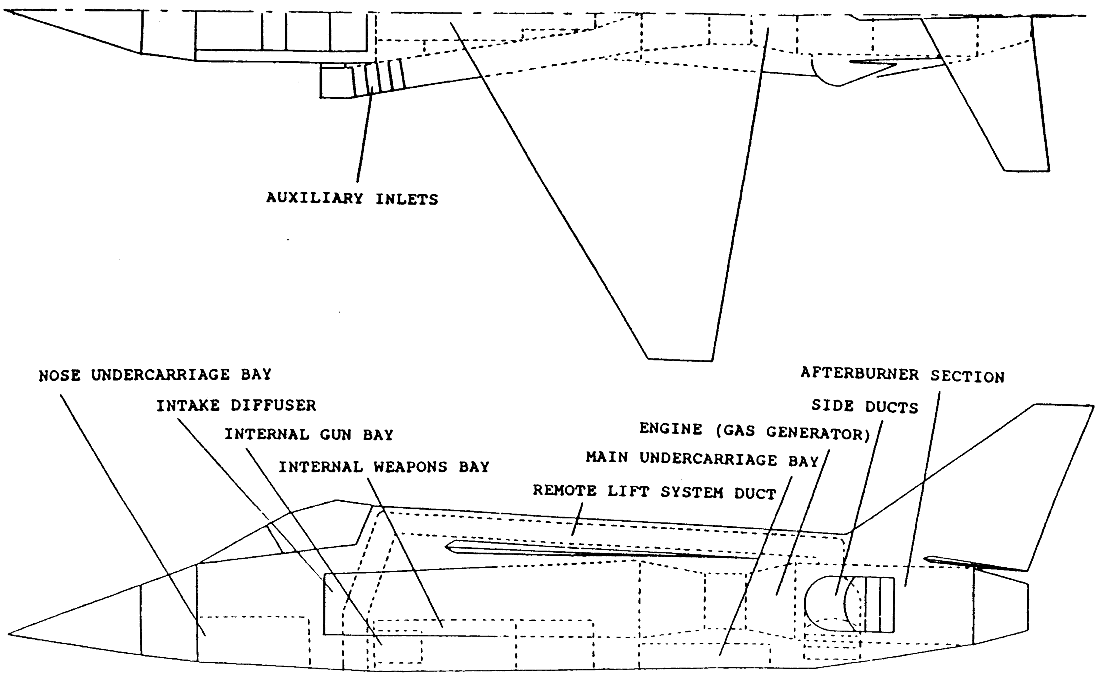

FIGURE 1. AIRCRAFT BASELINE CONFIGURATION

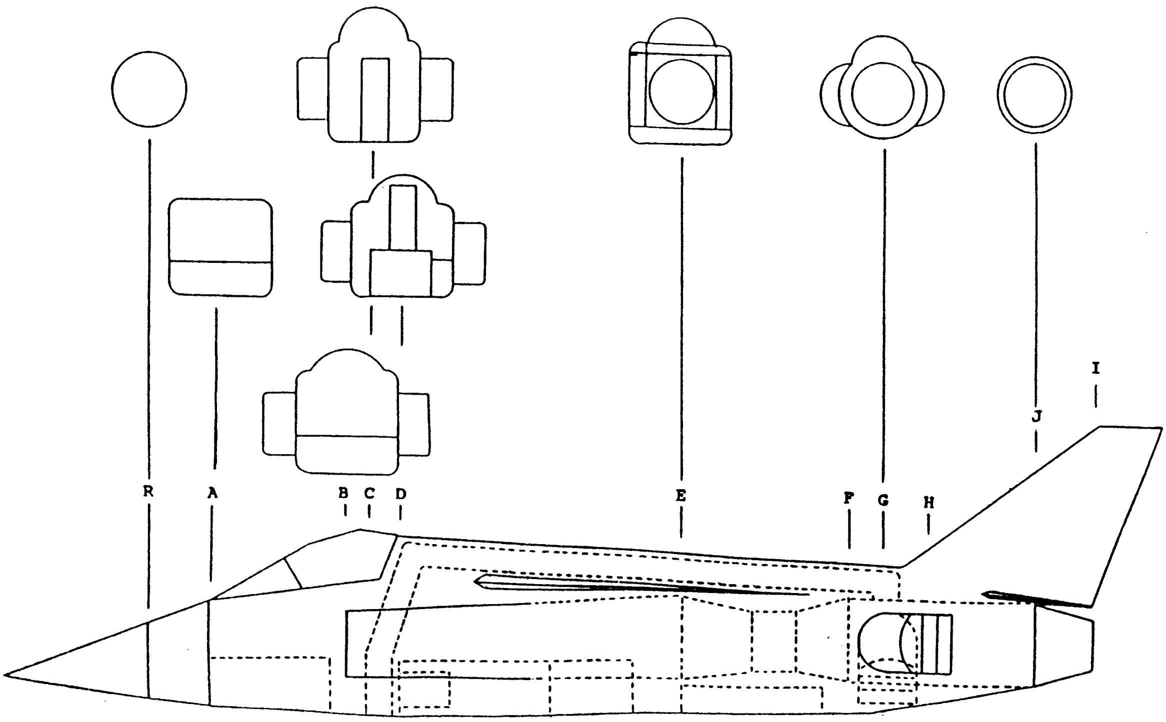

FIGURE 2. FUSELAGE STATIONS WITH CORRESPONDING SECTIONS

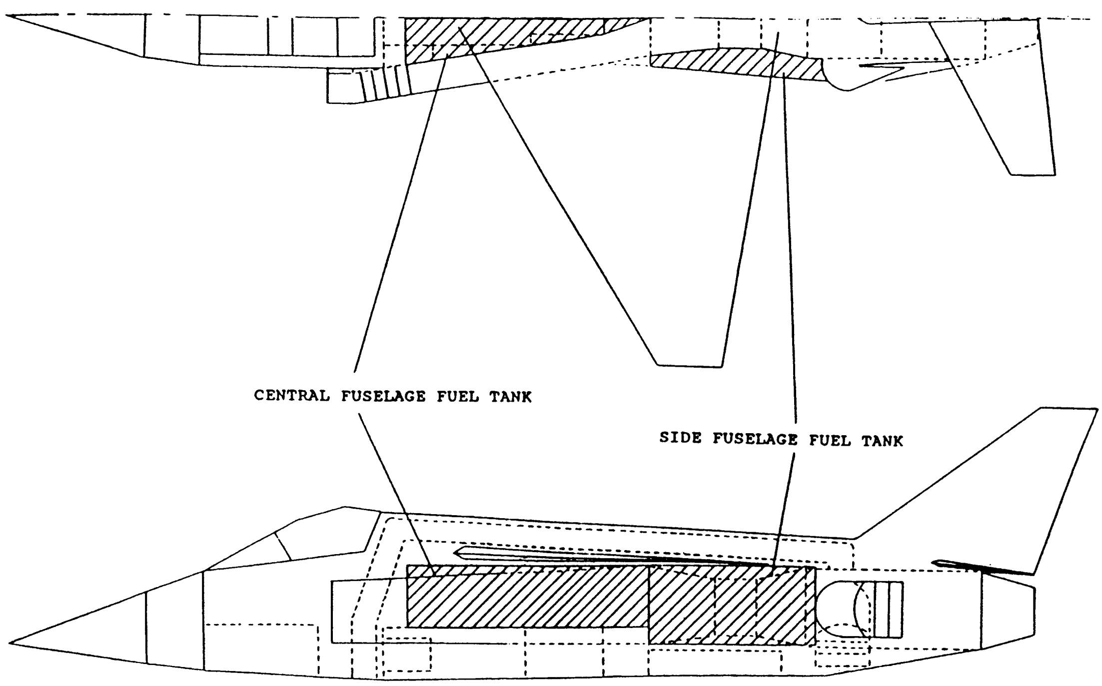

FIGURE 3. FUSELAGE FUEL TANK ARRANGEMENT

internally in a bay, placed between the RLS nozzle and the engine axially, and between the two intake diffusers laterally (Figs 1, 2). They are jettisoned by means of ejectors situated on the top of the bay. An internal gun is located in a bay on the left side of the weapons bay.

In addition to the wing fuel tanks, three fuselage tanks have been specified. A central fuel tank located above the internal weapons bay, ahead of the engine and between the intake diffusers, and two side tanks in either side of the engine gas generator (Fig.3). The side tanks have the same height as the engine at that position and blend with the side duct nozzles that follow them.

The initial baseline configuration defines an aircraft of around 19 t take-off weight and 20 m in length. The wing span is 13 m and the wing surface area is nearly 40 m^2. The engine maximum gross thrust at sea level conditions is 185 kN.

2.2. Design Synthesis

The design synthesis describes the aircraft baseline configuration in mathematical form, by means of semi-empirical and sometimes analytical design relationships.

Initially, using design input data, the sizing of the aircraft basic items is performed. Basic items are all the "standard" parts of the aircraft such as the radome, the cockpit, the undercarriage, the internal weapons bay, the internal gun bay, the intake diffusers, the engine, the RLS, the basic wing and the empennage. These parts are determined by input design data, and, in this sense, are considered basic items within the design synthesis. In the optimization, as it will be discussed later, many of these basic items may vary.

Next, the geometry of the aircraft is evaluated. Use of input design data is made taking into consideration the related basic items so that the aircraft can contain all the specified basic items. The fuselage geometry is evaluated at several stations along the fuselage with the help of a fairing curve, in order to define an acceptable aerodynamic shape, and area rule if required.

From the basic items and the geometry, the mass and the centre of gravity are calculated.

The aerodynamics follow, based on the geometry and the input aerodynamic data.

At the end, after having established all the characteristics of the aircraft, and using the sortie profile specifications (Table 1), the aircraft point performance is calculated.

SORTIE LEG No	SORTIE LEG DESCRIPTION
-	START-UP, TAXI, SHORT TAKE-OFF (30 s). CLIMB TO CRUISE ALTITUDE AND MACH NO.
1	CRUISE AT 10,000 m, M 0.7 FOR 400 km AT 1.0 g.
2	CRUISE AT 9,000 m, M 0.6 FOR 45 min AT 1.1 g. FIRE 2 AMRAAMS.
3	COMBAT AT 9,000 m, M 1.4, 1 TURN AT 3.0 g. FIRE 2 AMRAAMS.
4	COMBAT AT 1,000 m, M 0.8, 2 TURNS AT 8.0 g. FIRE 2 ASRAAMS, ALL AMMO. CLIMB TO CRUISE ALTITUDE AND MACH NO.
5	CRUISE AT 10,000 m, M 0.7 FOR 400 km AT 1.0 g.
-	HOVER FOR 30 s OUT OF GROUND EFFECT. VERTICAL LANDING WITH 5 % OF INTERNAL FUEL LEFT AT ENTRY TO HOVER.

TABLE 1. TYPICAL SORTIE PROFILE

2.3. Optimization

The optimization of the ASTOVL combat aircraft baseline configuration is carried out - by interfacing the aircraft design synthesis with an optimization code. The optimization code that was used is RQPMIN. This was developed by Skrobanski [12] and is one of a series of optimization codes used by DERA [13].

RQPMIN is a general numerical multi-variate optimization code. It is designed to solve constrained optimization problems, that is to minimize or maximize a function, subject to a number of constraints and upper and lower bounds imposed on designated variables.

The operation of RQPMIN is based on the Lagrange-Newton optimization. A stationary point of the Langrangian function is calculated by Newton's method. RQPMIN differs from similar codes in that it does not use a penalty or a criterion function to force global convergence. Instead, the concept of pseudo-feasibility is applied. A trial point is rejected if the square root of the sum of the squares of the constraints is greater than the radius of pseudo-feasibility.

RQPMIN involves in its operation external variables (EVs), independent variables (IVs), dependent variables (DVs), an objective function (OF), equality constraints (ECs) and inequality constraints (ICs). RQPM1N variables are the variables of the design synthesis code. EVs are design input variables. IVs are variables that are given an initial value and then are varied by RQPMIN. DVs are dependent on EVs and IVs. The OF is a design synthesis function chosen to be optimized by RQPMIN. ECs are specified equalities, involving design synthesis variables, that must be satisfied by the end of the optimization. ICs are similar to ECs with the difference that involve inequalities; they become active only if these inequalities are not satisfied. The selected IVs for this study are presented in Table 2.

IV No	IV DESCRIPTION
1	WING AREA
2	WING ASPECT RATIO
3	WING TAPER RATIO
4	WING QUARTER-CHORD SWEEP
5	WING THICKNESS-TO-CHORD RATIO
6	FRONT SPAR POSITION
7	REAR SPAR POSITION
8	WING POSITION
9	FIN QUARTER CHORD
10	TAILPLANE QUARTER-CHORD
11	ENGINE SCALE FACTOR
12	FUSELAGE LENGTH
13	FIRST FAIRING CURVE PARAMETER
14	SECOND " " "
15	THIRD " " "
16	FOURTH " " "
17	FIFTH " " "
18	SIDE FUEL TANK WIDTH
19	SIDE FUEL TANK ARM

TABLE 2. INDEPENDENT VARIABLES (IVs)

2.4. Objective Function (OF) Development

Although it has been suggested in a number of references that the aircraft take-off mass or the aircraft empty mass is the best OF, a number of other OFs were tried. This investigation aimed for an improved aircraft and this does not always mean an aircraft with lower empty mass. For example, an OF other than the empty mass may give an aircraft with the same empty mass but lower fuel mass. In search for a better OF, and since this type of aircraft is built "around the engine", the engine mass was next considered. In addition to the aircraft empty mass and the engine mass, four more OFs were tested; the engine scale factor, the wing area, the wing mass and the fuel mass.

It should be noted that the results of the OF investigation are not related to the baseline configuration optimization. This is because, for the purpose of the OF investigation, very light constraints were set which facilitate a convergence. Light constraint conditions were chosen to produce a more substantial reduction in OF investigation time and effort than would otherwise be needed.

3. Discussion of the Baseline Configuration Study Results

STOVL combat aircraft configurations are among the challenges in conceptual aircraft design, especially if a supersonic capability is also specified. The difficulties in evaluating such configurations are mainly due to the thrust-to-weight ratio needed, the matching of thrust and centre of gravity and the internal packaging constraints.

The requirements of a high thrust-to-weight ratio that is necessary for vertical landing - giving a long engine-and of an internal weapon bay with very long medium-range missiles, are conflicting. Several attempts were made to place the internal weapon bay in such a way as not to have the length of it added to the length of the engine. These failed, and therefore, the weapon bay remained ahead of, and in line with the engine.

Another major problem was the size of the RLS front duct. With a configuration that dictated an approximately 50 % thrust split between the front RLS duct and the rear engine side duct nozzles, a RLS duct of enormous cross-section became necessary. It was evident that a RLS duct of this size could not be accommodated in the aircraft fuselage. Two categories of alternatives were considered; the first was the non-circular cross-section duct and the second the multiple duct. Although many non-circular cross-sectional shapes provide satisfactory volume efficiency, they suffer from substantial pressure losses. In the multiple duct category the volume efficiency is almost as good, but at a small penalty in terms of increased frictional losses and weight. The selected solution was a RLS front duct composed of three circular ducts, one bigger in the middle and two smaller ones on either side. This three-duct arrangement is much smaller in height than a single circular duct of the same cross-section and, therefore, can fit in the upper part of the aircraft fuselage between the cockpit and the tail (Fig. 1). However, the matter requires further investigation.

Finally, the well known V/STOVL combat aircraft problem of engine hot gas ingestion [141, while hovering, was very briefly investigated with reference to the intake diffuser inlet position. Positioning of the inlet further back and away from the RLS front nozzle would either reduce the length of the intake diffuser unacceptably from the intake flow point of view, or would unnecessarily increase the aircraft length. The chosen alternative was to use auxilliary intakes in the upper surface of the diffusers, to be used in the hover. The forward flight intakes were chosen to be fixed in view of the Mach 1.6 maximum speed of the aircraft.

3.1. Discussion of the Design Synthesis

Although the design synthesis method developed by Lovell [4] was, in general, followed, significant changes were made. Most changes resulted from differences in the techniques used, and additions related to the specific ASTOVL configuration chosen. The basic item additions due to the ASTOVL configuration were related to the engine and the RLS. The engine thrust-to-weight ratio at landing was put to 1.15 (excluding bleed air for the reaction control system (RCS)). To this were added a 7 % allowance for the RCS [15] and an estimated 3 % due to RLS nozzle and duct, and engine swivelling duct losses. This brought the total thrust-to-weight ratio to 1.25. However, it should be pointed out that considerable variations exist for thrust losses; an example is the suckdown losses given as 13 % in Ref.15 and as 3 % in Ref.16.

The RLS presented many difficulties. Estimates had to be made to account not only for its structural but for its insulation mass as well. The structural mass calculation was based on comparisons with RALS (remote augmented lift system) concepts[17,18]. Willis, Konarski and Sutherland [19] being particularly useful. Although they dealt with ejector RALS, they provided useful size and mass information on ducts and nozzles.

The RLS nozzle position was examined in relation to the engine front/rear split. As very little room was available for nozzle movement due to the configuration (internal weapon bay), a 50 % thrust split was decided to provide a nozzle position between the cockpit front bulkhead and the internal weapon bay (Figs 1 and 2). A constant thrust split poses a limitation on the code, but a variable one would require transition stability limitation considerations that were beyond the scope of this work.

The fuselage geometry was evaluated with due care for the definition of the cross-sectional areas in question. The number of fuselage stations was greater than Lovell's [4], mainly because of the complicated rear fuselage. A lot of emphasis was placed on the determination of the fairing curve. It was made very clear that the fairing curve relates to the net cross-sectional area of the fuselage.

In general, Lovell's [4] tendency to use densities in mass calculations was not followed. Instead, actual mass values were preferred. It was felt that for items far away from the aircraft cg, an improved accuracy was particularly important for an ASTOVL aircraft. Lovell's [4] internal fuel tank solution was not adopted. The evaluation of the internal fuel volume capacity of the fuselage by way of subtracting the volume of the basic items from the fuselage volume has some drawbacks. The reason is that many parts of the fuselage are not suitable for fuel storage. Instead, three fuselage fuel tanks were designated, their location dictated by safety, reliability and aircraft cg limitations.

Only minor alterations have been made to Lovell's [4] drag estimation, but his lift-curve slope estimation was enhanced with interference effects. Preliminary calculations showed these effects to amount to around 10 % . For body and wing-body interference, the information available in Ref.20 was used, after being transformed into analytical form. An analytical expression for the tail interference downwash, based on finite wing theory, was derived from first principles [21].

The available engine performance module in data form took too much computing time and should be reconsidered. Perhaps a formula-based engine performance approach might be a better solution in the future.

3.2. Discussion of the Optimization and the Development of the Objective Function

A number of difficulties were encountered with the application of the optimization code RQPMIN, 1986 version, used in this study. The first is related to the tolerance limits of the code. RQPMIN [12] was designed for mathematical applications, and, its tolerance limits, the criterion as to whether the constraints have been satisfied or convergence achieved, were too small. Even their upper (maximum) value was inappropriate for engineering purposes. Numerous runs ended unsuccessfully because these tolerance limits could not be satisfied, even though they produced substantial reductions in the OF.

Another major problem was connected with the RQPMIN condition that all parameters, with the use of scale factors, should have been kept at values of around one. This was not always possible since during the optimization some parameters changed considerably.

During its feasibility steps, RQPMIN varied the IVs in every direction until it found a feasible path. When very tight constraints were specified, only four IVs exhibited variation during the optimization. They were the engine scale factor, the wing quarter-chord position, and the front and rear spar positions. Since the aircraft is built "around the engine" it is evident that the engine scale factor was the decisive parameter for the aircraft mass reduction. The aircraft mass reduction produces a shift in cg, and the wing quarter-chord position was used to control it. The spar position variation could not be explained.

It should be mentioned that RQPMIN lead to a much better optimization - empty mass reduction when convergence was not achieved; this occurred with the constraints being satisfied.

The constraint which drove the configuration was the thrust-to-weight ratio at landing. This constraint resulted in a large engine, and consequently, a large RLS. Both added substantially to the aircraft mass. Another significant constraint, deriving from the aircraft configuration, was the in-line positioning of the internal weapon bay and the engine. Again, this constraint added to the aircraft mass,, due to the resulting longer fuselage.

The most important performance constraints were those of the sustained turn rate, the specific excess power and the maximum Mach number (Table 3). The second sustained turn rate constraint proved impossible to achieve.

The closest to the constraint value of 9.5 deg/s at 9,000 m, M 0.9 and full engine power that could be achieved was around 4. In general, the specified performance constraints make a convergence very difficult. It seems that the

POINT PERFORMANCE PARAMETER	CONSTRAINT
ACCELERATION TIME FROM M 0.8 TO M 1.4 AT 9,000 m, MAX POWER	≤ 60 s
MAX MACH NO AT SEA LEVEL, MAX POWER	≥ 1.1
MAX MACH NO AT 11,000 m, MAX POWER	≥ 1.6
SPECIFIC EXCESS POWER AT M 0.9, SEA LEVEL, MAX POWER	≥ 300 m/s
SPECIFIC EXCESS POWER AT M 0.9, 9,000 m, MAX POWER.	≥ 150 m/s
SUSTAINED TURN RATE AT M 0.9, SEA LEVEL, MAX DRY POWER	≥ 12 deg/s
SUSTAINED TURN RATE AT M 0.9, 9,000 m, MAX POWER	≥ 9.5 deg/s
SUSTAINED TURN RATE AT M 1.4, 9,000 m, MAX POWER	≥ 6 deg/s
ATTAINED TURN RATE AT M 1.4, 9,000 m, MAX POWER	≥ 10 deg/s
RIDE QUALITY FACTOR AT 1,000 m, MAX POWER	≤ 5

TABLE 3. POINT PERFORMANCE CONSTRAINTS

	INITIAL CONFIGURATION	OPTIMIZED CONFIGURATION
LENGTH /m	20.0	19.774
WING AREA /m^2	40.0	40.142
ENGINE SCALE FACTOR	1.6	1.47
WEIGHTS /kg		
FUSELAGE	3049.8	3272.3
WING	2512.3	3501.7
TAILPLANE	409.0	229.0
FIN	1725.8	756.0
ENGINE	3770.6	3501.2
EMPTY	14421.1	14213.7
FUEL	5240.1	3786.2
TAKE-OFF	20561.7	18900.4

TABLE 4. OPTIMIZED VERSUS INITIAL CONFIGURATION DATA

COLUMN	1	2	3	4	5	6	7	8	9	10	11
OBJ FUN	INIT CONF	A/C EMPT M	ENG M	ENG M	ENG M	ENG M	ENG M	RTP	SW	MWC	MTGFI
ENGINE M	3570.4	2599.7	2598.0	2640.1	2603.3	2602.2	2597.6	2597.5	2609.4	2638.0	2759.3
FUEL M	4570.0	3094.1	3033.1	3058.6	3027.0	3029.8	3016.3	3015.7	2948.4	3160.4	2906.7
FUSELAGE M	2735.0	2192.6	2195.8	2244.5	2211.8	2191.6	2191.0	2190.0	2191.4	2324.6	2330.8
WING M	2286.4	999.6	1055.3	1164.0	1064.8	1026.5	1019.5	1019.6	1094.7	1008.9	1607.1
EMP TAIL M	476.0	199.2	199.8	206.0	200.5	198.4	196.5	196.5	195.6	206.1	209.7
EMP FIN M	1812.1	628.4	641.3	656.1	643.4	628.7	619.6	619.9	608.0	627.0	586.4
SUM ABOVE	15449.5	9713.6	9723.3	9969.3	9750.8	9674.6	9640.5	9638.6	9647.5	9965.0	10400.0
A/C EMPTY M	13830.8	9564.7	9635.4	9893.0	9569.0	9598.8	9569.3	9568.4	9643.8	9750.0	10438.8
A/C TAKE-OFF M	19301.3	13559.3	13569.0	13852.1	13596.5	13520.1	13486.1	13484.6	13492.7	13810.9	14246.0
ENG SCALE F	1.50000	1.02348	1.02267	1.04300	1.02520	1.02485	1.02248	1.02239	1.02813	1.04193	1.10076
A/C LENGTH	17.8000	14.9264	14.9239	14.9871	14.9318	14.9306	14.9233	14.9230	14.9409	14.9691	15.1633
WING AREA	35.0000	23.2766	23.3737	23.8597	23.4466	23.1786	23.1150	23.1103	23.0502	23.8663	24.1958
CONVER	-	B	B	MX ITER	A	NO F PR	A	A	B	NO F PR	B
ITER NO	-	7700	5700	8000	16000	5100	6600	8800	8500	6700	5500
NOTES	-	XTOLV, XTOLU 0.001	CONST 5 NOT REL	CHANGED IN COND	CONST 5 NOT REL	XTOLV, XTOLU 0.00001 CHANGED IN COND	XTOLV, XTOLU 0.001	XTOLV, XTOLU 0.001	XTOLV, XTOLU 0.001	XTOLV, XTOLU 0.001	XTOLV, XTOLU 0.001

TABLE 5. OPTIMIZATION OBJECTIVE FUNCTION DEVELOPMENT RESULTS

	COX AND ROSKAM (Ref.15)	YAK-141 (Ref.23)	CoA KEHAYAS (Ref.2)	CoA S-95 (Ref.22)
LENGTH /m	16.8	18.4	19.8	18.3
SPAN /m	10.1	10.1	12.6	12.1
WING AREA /m^2	29.0	37.0	40.1	48.6
SL MAX SPEED	1.4	1.0	1.1	1.2
COMBAT RADIUS /km	520	690	400	440
CRUISE/LIFT ENGINE SL THRUST /kN REHEAT	158	152	272	
DRY		108	195	
DEDICATED LIFT ENGINE SL THRUST /kN	54	80	-	-
PROPULSION SYSTEM TOTAL WEIGHT /kg	2785		3500	
FUEL WEIGHT /kg	3920	6150	3790	5600
EMPTY WEIGHT /kg	9580	11650	14210	12440
TAKE-OFF WEIGHT /kg	14200	19500	18900	19000

TABLE 6. COMPARISON OF ASTOVL DESIGNS

optimizer needs some freedom in order to converge. Furthermore, it is evident that some of the performance constraints contradict each other.

From the purely optimizational point of view the most difficult constraints were the ECs, because the tolerance problem discussed earlier was much more acute than in the ICs. The explanation lies in the fact that an equality is approached from both sides; an inequality from one. A way to by-pass this difficulty might be to replace every EC with two ICs, thus allowing whatever tolerance is considered appropriate. The results of the optimization of the baseline configuration are shown in Table 4. Both the initial and the optimized configuration satisfied the specified constraints.

In the search for a better OF, the aircraft take-off mass was used as a measure of comparison. In the course of the investigation, six aircraft parameters - empty mass, engine mass, engine scale factor, wing surface area, wing mass, and fuel mass - were tried as OFs. The results are shown in Table 5. Starting with the engine mass as OF, and after a number of different sets of initial conditions., only marginally better results were achieved. At best, the aircraft take-off mass was reduced by 73 kg or 0.54 % (Table 5, column 7). This slight improvement derived mainly from fuel mass reduction,,- while the empty mass is 0.05 % worse than the empty mass OF case. Next. the engine scale factor was tried as OF, as analternative to engine mass, but with similar results (Table 5, column 8). During these trials,, a tendency for wing mass to increase was observed. Thus. wing surface area and wing mass were set as OFs. Wing surface area gave similar results, but wing mass was much worse (Table 5, columns 9 and 10). The last attempt was with fuel mass but without success (Table 5, column 11).

Consequently, engine mass, engine scale factor and wing surface area gave, as OFs, slightly better results than empty weight, but from the engineering point of view this improvement could only be regarded as nominal. A more realistic approach would be to investigate the minimum acquisition or life-cycle costs, but this was beyond the scope of this study.

4. Comparison with Similar ASTOVL Designs

The optimized baseline configuration was compared with three other ASTOVL designs, as shown in Table 6. Two are case studies; the one by Cox and Roskam [15] and the other the Cranfield College of Aeronautics design project S-95 [22]. The third is the Russian experimental ASTOVL fighter, the YAK-141 [23].

All four designs are of the remote lift type, with Cox and Roskam and YAK-141 having separate lift engines. The YAK-141 figures are for STO operation.

From what it can be deduced, especially for the YAK-141, all four designs have similar mission profiles, performance and weapons. As shown in Table 6. three out of the four designs (the YAK-141, the CoA S-95 and the present) have comparable dimensions and weights.

Some differences exist in the wing area, fuel and empty weight figures. The CoA S-95 has a larger wing area and the present design a higher empty weight. The higher empty weight of the present design can be attributed to its complex powerplant configuration. A reason for the larger S-95 wing area was its blended nature and edge-alignment, to improve its stealth characteristics. The YAK-14 and S-95 exhibit

significantly higher fuel consumption. YAK-141 fuel consumption must be a result of its much higher payload, and, to a lesser extent, combat radius.

The Cox and Roskam design is much smaller in every respect. The most obvious explanation may be that the structural weight of this design was underestimated [15].

Separate lift engine designs tend to have lower empty weight.

5. Concluding Remarks

The baseline configuration, the design synthesis and the optimization of the baseline configuration of an ASTOVIL combat aircraft have been performed.

The baseline configuration represents an advanced supersonic STOVL combat aircraft with an internal weapon bay and a remote lift system for landing.

The design synthesis code describes the baseline configuration and provides a fast computation of the aircraft geometry, mass. aerodynamics and performance. It is modular in form and can be easily modified to incorporate different methods and techniques, and to account for other configurations. Every effort has been made to strike a good balance between the various parts of the code in relation to the detail of the techniques used, but further consideration is needed.

The interfacing of the design synthesis code with the optimizer RQPMIN and the optimization of the baseline configuration were successfully achieved. The optimizer RQPMIN exhibits some functional problems, for which further attention is required. The specified point performance constraints were very tight, and as a result the second sustained turn rate constraint could not be satisfied. The best objective function for the reduction of the aircraft take-off mass was found to be either the aircraft empty mass or the engine mass.. The optimized baseline configuration is a 19.8 m long, 18.9 t take-off weight aircraft.

Comparison with other ASTOVL designs indicated considerable similarities. However. the comparison suggested that separate lift engine designs tend to have lower empty weight. Therefore. from the design point of view, without taking into account operational, maintenance or logistic aspects, a separate lift engine might be a better solution than a RLS.

References

[1] Tamplin G C, Hammond D L and Fredette R E. Next-generation STOVL fighter. Aerospace *Engineering, pp 15-20,* January 199 1.

[2] Kehayas N. ASTOVL combat aircraft design synthesis and optimization. *Ph.D. Thesis. Cranfield Institute of Technology,* 1992.

[3] Collingbourne J. Multivariate optimization applied to the initial design of transport *aircraft. RAE Technical Report 84044, 1984.*

[4] Lovell D A. The application of multivariate optimization to combat *aircraft* design. *RAE Technical Report* 88003, January 1988.

[5] Serghides V C. Design synthesis for canard-delta combat aircraft. Ph.D. Thesis, Cranfield Institute of Technology, 1988.

[6] Siegers F and Smith H. Numerical synthesis methodology for conceptual design of new generations of combat aircraft. AIAA Paper 95-3881, 1995.

[7] Fozard J W. Tactical jet V/STOVL Its future in a CTOL world. SAE *Paper* 861637, October 1986.

[8] Brown D M. Supersonic STOVL conceptual design of a fighter attack aircraft. *AIAA Paper* 89-2112, 1989.

[9] Levine J and Inglis M. US/UK advanced short take-off and vertical landing (ASTOVL) program. *AIAA Paper* 89-2039, 1989.

[10] Schrage D P and Meyer S A. VTOL operational considerations and their impact on future military design requirements. *AIAA Paper* 86-2649, 1986.

[11] Ward B D and Lewis W J. Advantages of thrust vectoring for STOVL. *AIAA Paper* 87-1708, 1987.

[12] Skrobanski J J. User guide for RQPMIN. *RAE Technical Memorandum* AERO 2059, January 1986.

[13] Smith J S and Lee C A. The RAE combat aircraft multi-variate optimization. *AIAA Paper* 89-2080, 1989.

[14] McLemore H C and Smith C C. Hot gas ingestion of large-scale jet VTOL fighter type models. *NASA TN* D-4609, 1968.

[15] Cox B and Roskam J. Preliminary design of a supersonic short take-off and vertical landing (STOVL) fighter aircraft. *AIAA Paper* 90-3231, 1990.

[16] Raymer D P. The impact of VTOL on the conceptual design process. *AIAA Paper* 88-44798, 1988.

[17] Sammuels J J and Hahn A S. A parametric approach to hover balance analysis of two STOVL fighter concepts. *SAE Paper* 861631, October 1986.

[18] Scott M L. S-80 roll control and remote augmented lift systems. *MSc. Thesis, Cranfield Institute of Technology,* 19 8 1.

[19] Willis W S, Konarski M and Sutherland M V. Conceptual design, evaluation and research identification for remote augmented propulsive lift systems (RALS) with ejectors for VTOL aircraft. *NASA* CR-167906, .1983.

[20] *USAF stability and control.* McDonnell Douglas Corporation, 1975.

[21] Hoerner S F and Borst H V. *Fluid-dynamic* lift. Published by the author, 1975.

[22] Smith H. Systems design for an advanced short take-off and vertical landing combat aircraft. *Aircraft Engineering and Aerospace Technology, Vol* 69, No 2, pp 129-144,1997.

[23] World *Aircraft and Systems Directory* 1996/1997, Brassey's, 1996.